

# Data-driven modeling of multiscale phenomena with applications to fluid turbulence

Brandon Choi<sup>1</sup>, Matteo Ugliotti<sup>1</sup>, Mateo Reynoso<sup>1</sup>, Daniel R. Gurevich<sup>2</sup>, and Roman O. Grigoriev<sup>1\*</sup>

<sup>1</sup>*School of Physics, Georgia Institute of Technology, Atlanta, GA 30332, USA* and

<sup>2</sup>*Department of Mathematics, University of California, Los Angeles, CA 90095, USA*

(Dated: November 14, 2025)

This letter introduces a novel data-driven framework for constructing accurate and general equivariant models of multiscale phenomena which does not rely on specific assumptions about the underlying physics. This framework is illustrated using incompressible fluid turbulence as an example that is representative, practically important, reasonably simple, and exceedingly well-studied. We use direct numerical simulations of freely decaying turbulence in two spatial dimensions to infer an effective field theory comprising explicit, interpretable evolution equations for both the large (resolved) and small (modeled) scales. The resulting closed system of equations is capable of accurately describing the effect of small scales, including backscatter—the flow of energy from small to large scales, which is particularly pronounced in two dimensions—which is an outstanding challenge that, to our knowledge, no existing alternative successfully tackles.

*Introduction*—Construction of mathematical models of physical systems—at length, time and, energy scales of interest—has long stood at the foundation of physics. This cornerstone paved the way to improving our understanding of the physical world and making numerous groundbreaking predictions. Often, a *fundamental theory* is available which provides an exact description of the microscopic details but is practically intractable or fails to generate the needed insight at the scales of interest. In such cases, it is desirable to construct an *effective field theory* that only describes the relevant degrees of freedom at the scales of interest without trying to model microscopic details. Effective theories are commonly used in particle, nuclear [1], and condensed matter physics [2], but examples such as the Chapman-Enskog theory [3] are found in classical physics as well.

A top-down effective theory can be derived formally from the corresponding fundamental theory only in very specific limits, e.g., the Chapman-Enskog theory requires the gas to be near local thermodynamic equilibrium and the Knudsen number (characterizing the mean free path) to be small. However, one can ask whether a sufficiently general approach exists that, at least in some classes of problems, allows an effective theory to be inferred in a systematic way from the corresponding fundamental theory. A particular class of problems where this capability would be most welcome involves multiscale phenomena, such as turbulence in fluids and plasmas, which can feature structures with length and time scales varying by tens of orders of magnitudes.

Consider, for instance, Newtonian fluids which are well-described by the continuity and Navier-Stokes (momentum) equations

$$\nabla \cdot \mathbf{u} = 0, \quad (1a)$$

$$\partial_t \mathbf{u} + \mathbf{u} \cdot \nabla \mathbf{u} = -\nabla p + \nu \nabla^2 \mathbf{u}, \quad (1b)$$

where  $\nu$  is the kinematic viscosity, down to the scale of microns. The momentum equation features a nonlinearity which both gives rise to the multiscale nature

of turbulent flows [4] and severely complicates analysis. Furthermore, this multiscale nature of turbulence makes solution of the fundamental transport equations via direct numerical simulations (DNS) infeasible in practical applications. In particular, the ratio between the largest and smallest length scales in three-dimensional turbulence scales as  $M \propto \text{Re}^{3/4}$ , where  $\text{Re}$  is the Reynolds number, while fully resolved DNS requires solving equations for  $M^3$  degrees of freedom at each time step. For instance, atmospheric jet flows and oceanic currents are described by  $\text{Re}$  ranging between  $10^{10}$  and  $10^{12}$ , which corresponds to  $10^{22} \lesssim M^3 \lesssim 10^{27}$ .

To circumvent this limitation, various models of fluid turbulence have been introduced which involve either temporal or spatial coarse-graining as in, respectively, the Reynolds-averaged Navier-Stokes (RANS) or large eddy simulation (LES). While the coarse-graining procedure itself is formal and general, the equations describing the averaged fields and their fluctuations cannot be closed without making specific assumptions, yielding a *phenomenological description*. In the case of both RANS and LES, an additional *closure* term appears in the momentum equation. It represents the effect of the small (modeled) scales on the large (resolved) ones and its functional form is assumed based on various empirical arguments rather than derived.

For instance, in LES, the velocity and pressure fields are decomposed into the large- and small-scale components,  $\phi = \bar{\phi} + \phi'$ , using the filtering operator

$$\bar{\phi} \equiv \mathcal{F}(\phi) \equiv \int d\mathbf{r}' G_\Delta(\mathbf{r} - \mathbf{r}') \phi(r'), \quad (2)$$

where  $\Delta$  is the cutoff length scale that defines the resolution of the resulting coarse-grained description. Applying this operator to the fundamental model (1), one obtains a pair of equations for the large-scale components

$$\nabla_i \bar{u}_i = 0, \quad (3a)$$

$$\partial_t \bar{u}_i + \bar{u}_j \nabla_j \bar{u}_i = -\nabla_i \bar{p} + \nu \nabla^2 \bar{u}_i - \nabla_j \tau_{ij}, \quad (3b)$$

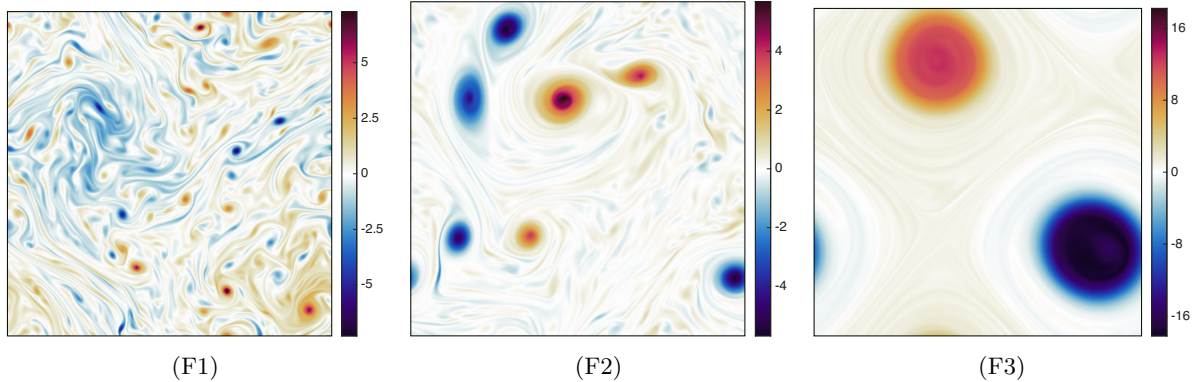


FIG. 1: Representative flow fields used to generate the test data. Shown is the vorticity field.

where we use Einstein implicit summation notation. The closure term  $-\nabla_j \tau_{ij}$  is expressed via the subgrid-scale (SGS) stress tensor  $\tau_{ij} = \overline{u_i u_j} - \bar{u}_i \bar{u}_j$ , which generally cannot be expressed in terms of the resolved fields (here,  $\bar{u}$  and  $\bar{p}$ ) and thus requires modeling.

A variety of phenomenological models, each with its strengths and weaknesses, have been proposed. Among the most widely used models are those based on the eddy viscosity hypothesis such as the Smagorinsky model [5] and its dynamic version [6, 7]. Another popular type are the similarity models [8, 9]. Models of both types, as well as hybrids thereof (e.g., the dynamic mixed model [8]) perform well on some benchmarks [10]. However, they are all based on physical assumptions—such as statistical homogeneity, isotropy, and scale invariance—and struggle when these assumptions break, e.g., in the presence of coherent structures. Recent development of data-driven approaches has led to a flurry of efforts to construct closures as functions of the resolved fields by leveraging high-fidelity DNS data. However, only a small fraction of those studies were aimed at obtaining an explicit functional form of the relation, as opposed to black-box relations encoded by neural networks (see, e.g., [11]). Examples include approaches based on sparse regression (e.g., random forest regression [12], sequential thresholding ridge regression [13], relevance vector machine [14]), symbolic regression (e.g., genetic expression programming [15, 16]) or a combination of symbolic and sparse regression [17]. However, none of the data-driven models outperform the leading phenomenological models.

Coherent structures can be very prominent in some types of turbulent flows, e.g., those that are effectively two-dimensional. Such flows often feature strong local fluxes of energy from small to large scales. For a variety of reasons, no existing SGS models—phenomenological or data-driven—are capable of correctly describing backscatter, which plays a key role in a variety of physical phenomena. One prominent example is transport of angular momentum in accretion disks, where magnetorotational instability that takes place at small scales cru-

cially affects the large scales. Although efforts to develop an LES-like description of scale interaction in the context of magnetohydrodynamics have been made [18], proper treatment of backscatter in this and other contexts remains an open problem.

This letter introduces a general data-driven framework for inferring an effective field theory of multiscale phenomena from the underlying fundamental description. This framework requires no specific phenomenological assumptions and ensures that the resulting theory is equivariant and interpretable. Unlike the bulk of SGS models, the dynamics of small scales and scale interaction are characterized explicitly, which enables an accurate description of backscatter in the case of fluid turbulence.

*Methodology*—We will retain the coarse-graining approach used in LES to separate the degrees of freedom with length scales larger and smaller than an arbitrary cutoff scale  $\Delta$ . The choice of the kernel  $G$  in equation (2) is partly arbitrary but must satisfy a number of constraints such as locality in physical and Fourier space [19, 20]. We use a normalized Gaussian kernel (with second moment  $\sigma^2 = \Delta^2/12$ ) exclusively in this letter as it maximizes locality in both spaces. To make the description finite-dimensional (e.g., to enable numerical solution), we additionally apply a sharp spectral filter, which cuts off scales past  $\Delta$ , making the combined filter non-invertible. The resulting splitting formally defines the governing equations for both large scales (here the system (3)) and small scales. The variables describing small scales and the associated governing equations are discarded in LES—which leads to the problems discussed previously—but are occasionally retained in RANS. In the latter case, the effect of small scales is represented by an SGS stress tensor whose formal evolution equation [21] includes variables other than  $\bar{u}_i$ ,  $\bar{p}$  and  $\tau_{ij}$ , generated by the nonlinearity, so that the resulting system of equations is not closed.

Construction of a *closed* system of equations requires identifying (1) proper variables describing small scales, (2) approximate governing equations for these variables,

and (3) an approximate constitutive relation for the SGS tensor. While it is natural to expect the small scales to be described by additional tensor field(s) with their own evolution equation(s), the choice of these fields is not obvious *a priori*. The SGS tensor itself is generally a poor choice, as it also contains substantial contributions from the large scales. This can be seen easily by considering the exact Galilean-invariant decomposition [22, 23]

$$\tau_{ij} = L_{ij} + C_{ij} + R_{ij} \quad (4a)$$

$$L_{ij} = \overline{\bar{u}_i \bar{u}_j} - \bar{\bar{u}}_i \bar{\bar{u}}_j \quad (4b)$$

$$C_{ij} = \overline{\bar{u}_i u'_j + u'_i \bar{u}_j} - \bar{\bar{u}}_i \bar{u}'_j - \bar{u}'_i \bar{\bar{u}}_j \quad (4c)$$

$$R_{ij} = \overline{u'_i u'_j} - \bar{u}'_i \bar{u}'_j \quad (4d)$$

of the SGS tensor into the Leonard ( $L$ ), Reynolds ( $R$ ), and cross ( $C$ ) stress tensors describing, respectively, the interaction of large scales, interaction of small scales, and interscale interaction. While both  $\mathbf{u}$  and  $\mathbf{u}'$  (and thereby  $L$ ,  $C$  and  $R$ ) can be reconstructed from  $\bar{\mathbf{u}}$  exactly for the Gaussian filter, the sharp spectral filter is not invertible and so some of the tensors may not be accurately described in terms of the resolved fields.

Both the governing equations for the small-scale variables and the constitutive relation for the SGS stress tensor can be inferred using a data-driven approach. Specifically, we use the SPIDER framework [24] which has been thoroughly validated by recovering fundamental models describing active nematics [25], turbulent channel flow [26], and turbulent convection [27]. SPIDER combines group representation theory, weak formulation of differential equations, and sparse regression to infer complete equivariant models, including boundary conditions, directly from data (experimental or numerical).

SPIDER searches for sparse relations explicitly equivariant with respect to a relevant symmetry group. This is done systematically and comprehensively by exploring search spaces corresponding to different irreducible representations. For instance, for the rotation group, each search space is defined by a basis set of tensors  $\{F_k^1, F_k^2, \dots\}$  that transform according to an irreducible representation  $k$  and are constructed using contractions and tensor products of the variables (e.g.,  $\bar{u}_i, \bar{p}, \dots$ ) and their derivatives (e.g.,  $\partial_t \bar{u}_i, \nabla_i \bar{p}, \nabla_j \bar{u}_i, \dots$ ). The tensor libraries  $\mathcal{L}_k = \{F_k^1, \dots, F_k^{N_k}\}$  are then finitely truncated by selecting an upper bound on the *complexity* of terms, typically defined as the number of variables and differential operators appearing in a given term. In this way, multiple physical relations can be identified in the form

$$c_1 F^1 + \dots + c_N F^N = 0, \quad (5)$$

where  $c_n$  are learned constant coefficients.

In this letter, we consider non-relativistic flows, so the relevant symmetries include translations, rotations, and Galilean transformations. For simplicity, we consider only the integer-rank tensor (not spinor) representations

of the rotation group. Evaluating equation (5) in weak form over a collection of spatiotemporal regions yields an overdetermined linear system  $Q\mathbf{c} = 0$  which is solved to find an approximate sparse solution  $\mathbf{c} = (c_1, \dots, c_N)$ . Depending on the objective, one can either require  $|\mathbf{c}| = 1$  (homogeneous regression) or  $c_m = 1$  for some  $1 \leq m \leq N$  (inhomogeneous regression). Finally, the scaling of the coefficients with parameters (here,  $\Delta$  and  $\nu$ ) is inferred through dimensional analysis and verified by generating data for a range of parameters.

We consider two-dimensional turbulence, which features pronounced coherent structures (eddies) that break statistical isotropy/homogeneity as well as strong backscatter [28], making it an ideal testing ground. We use a pseudospectral solver [11] to generate fully resolved DNS data on a square domain of size  $\ell = 2\pi$  with periodic boundary conditions. Figure 1 shows snapshots of such flows representing the inverse cascade (F1), freely decaying turbulence (F2) and the direct cascade (F3) used as initial conditions. For each of the three initial conditions, a numerical solution corresponding to  $O(1)$  eddy turnover time is generated for each value of the viscosity corresponding to Reynolds number  $Re = u_{rms} \ell / \nu$  equal to  $10^4$ ,  $10^5$ , and  $10^6$  on computational grids with respective resolutions of  $2048^2$ ,  $4096^2$ , and  $4096^2$ . Next, coarse-grained datasets are generated by applying the filtering operator for a range of cutoff scales  $\Delta$ . Finally, equations are inferred from the coarse-grained data using the Python implementation of SPIDER [24].

*Results*—To determine whether the SGS stress tensor can be represented by functions of the resolved fields  $\bar{\mathbf{u}}$  and  $\bar{p}$ , we use them to construct the respective rank-0 and symmetric trace-free rank-2 libraries and employ inhomogeneous regression. Across all data sets we consistently find

$$\tau_{ij} \approx c_1 \nabla_k \bar{u}_i \nabla_k \bar{u}_j + c_2 \nabla_k \nabla_m \bar{u}_i \nabla_k \nabla_m \bar{u}_j, \quad (6)$$

where the second right-hand-side term is generally small compared to the first one. Incidentally, this result corresponds to the formal series expansions of  $L + C$  in powers of  $\Delta$  [20]. Using dimensional analysis and the numerical values of the coefficients identified by SPIDER, we find  $c_1 = \Delta^2/12$  and  $c_2 = \Delta^4/288$ , consistent with the coefficients of the formal expansion.

On the other hand, the tensor  $R$ , which is generally small compared with  $L$  and  $C$ , cannot be expressed in terms of  $\bar{\mathbf{u}}$  or  $\bar{p}$  with even moderate accuracy. Therefore, we simply treat  $R$  as an additional variable in the effective field theory, one that describes small scales, and parameterize the SGS tensor as

$$\tau_{ij} \approx \frac{\Delta^2}{12} \nabla_k \bar{u}_i \nabla_k \bar{u}_j + \frac{\Delta^4}{288} \nabla_k \nabla_m \bar{u}_i \nabla_k \nabla_m \bar{u}_j + R_{ij} \quad (7)$$

which we refer to as the LCR model. This model not only reproduces the individual components of the SGS

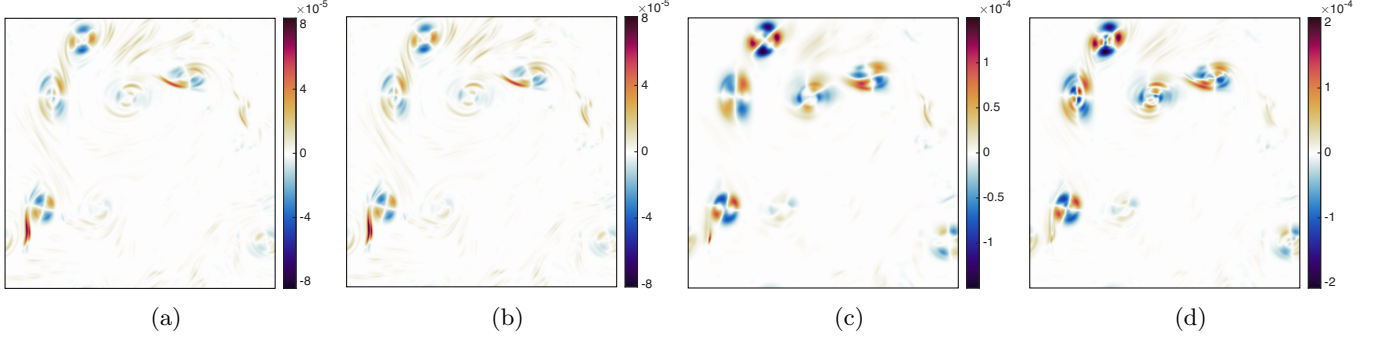


FIG. 2: Representative snapshot of the energy flux  $\Pi$  for DNS (a), the LCR model (b), DS model (c), and DM model (d) for the flow F2 at  $Re \sim 10^6$  and cutoff scale  $\Delta = \ell/64$ .

stress tensor faithfully but also accurately captures the spatiotemporal structure of the energy flux  $\Pi \equiv -\tau_{ij} \bar{S}_{ij}$  (where  $S_{ij}$  denotes the symmetric part of  $\nabla_i u_j$ ) *including* backscatter (regions where  $\Pi < 0$ ). This is illustrated in figure 2 for the freely decaying flow F2. For reference, the figure also shows the predictions of the widely used dynamic Smagorinsky (DS) model as well as the dynamic mixed (DM) model (see End Matter), which is considered to be one of the most accurate LES models [29]. Both phenomenological models fail to predict local fluxes.

The inclusion of  $R$  as a new field requires an additional governing equation in order to close the system. This equation can be inferred using rank-0 and symmetric trace-free rank-2 libraries constructed from  $\bar{u}_i$ ,  $\bar{p}$ , and  $R_{ij}$ . We robustly discover an evolution equation of the form

$$\begin{aligned} \partial_t R_{ij} = & c_1 \bar{u}_k \nabla_k R_{ij} + c_2 (R_{ik} \nabla_k \bar{u}_j + R_{jk} \nabla_k \bar{u}_i) \\ & + c_3 \nabla^2 R_{ij} + c_4 R_{ij}. \end{aligned} \quad (8)$$

Using a combination of dimensional analysis and numerical values of the coefficients for different data sets, we find  $c_1 = -1$ ,  $c_2 = 1$  and  $c_3 = \nu$ . For  $c_4$ , we find that it has both dimensions and numerical values consistent with the inverse of the eddy turnover time, exhibiting no clear dependence on the parameters  $\nu$  and  $\Delta$ . Therefore, we relax the assumption of translational invariance made by SPIDER that requires  $c_4$  to be independent of position and time and take it to be a function of the resolved flow. For instance, in the inviscid limit, rescaling the velocity of the initial condition by a constant factor changes the inverse time scale and, hence,  $c_4$  by the same factor, so  $c_4$  should be linear in  $\bar{u}$ . Because  $c_4$  is a scalar, it should be expressible as a function of the energy  $E = u_i u_i/2$  as well as the invariants of the tensor  $\nabla_i \bar{u}_j$  [30]; in 2D, these are given by  $|\bar{S}| = \sqrt{2 \bar{S}_{ij} \bar{S}_{ij}}$  and  $|\bar{\Omega}| = \sqrt{2 \bar{\Omega}_{ij} \bar{\Omega}_{ij}}$ , where  $\Omega_{ij}$  is the antisymmetric component of  $\nabla_i u_j$ . Dimensional arguments would then require  $c_4 = \Delta^{-1} \sqrt{E} f(\Delta |\bar{\Omega}|/\sqrt{E}, \Delta |\bar{S}|/\sqrt{E}, \dots)$ , where  $f$  is an arbitrary function. A general relation of this form can be inferred from the data using, e.g., symbolic regres-

sion. However, a good approximation can be found using a series expansion of  $f$ :

$$c_4 = \alpha_1 |\bar{S}| + \alpha_2 |\bar{\Omega}| + \alpha_3 \Delta^{-1} \sqrt{E} + \dots, \quad (9)$$

where  $\alpha_j$  are non-dimensional coefficients. Sparse regression yields  $c_4 \approx -|\bar{S}|/2$ . Collecting everything, we find

$$\begin{aligned} \partial_t R_{ij} + \bar{u}_k \nabla_k R_{ij} = & R_{ik} \nabla_k \bar{u}_j + R_{jk} \nabla_k \bar{u}_i \\ & + \nu \nabla^2 R_{ij} - \frac{1}{2} |\bar{S}| R_{ij} \end{aligned} \quad (10)$$

To measure the accuracy in predicting a tensor variable, we will employ a magnitude-aware correlation

$$\mathcal{C}(A, B) = \frac{\langle A_{ij} \dots B_{ij} \dots \rangle}{\max(\langle A_{ij} \dots A_{ij} \dots \rangle, \langle B_{ij} \dots B_{ij} \dots \rangle)} \quad (11)$$

between tensor fields  $A$  (ground truth) and  $B$  (prediction), where  $\langle \cdot \rangle$  denotes spatial averaging, with  $\mathcal{C}(A, B) = 1$  only when  $A = B$ . Using  $C_R = \mathcal{C}(\partial_t R_{\text{DNS}}, \partial_t R_{\text{LES}})$  as a metric, we find equation (10) to accurately describe all flow regimes for sufficiently small  $\Delta$  (cf. figure 3). As expected, the accuracy deteriorates as  $\Delta$  approaches the scale of coherent structures, since the coarse-grained description is not meant to model these.

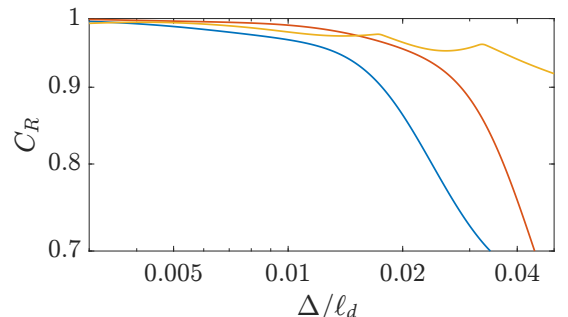


FIG. 3: The accuracy of the evolution equation (10), quantified by the correlation  $C_R$ , as a function of  $\Delta/\ell$  for F1 (blue), F2 (orange) and F3 (yellow) at  $Re = 10^6$ .

*Conclusions*—Taken together, the closed system of equations (3), (7) and (10) defines an effective field theory which describes incompressible fluid turbulence up to

the cutoff scale  $\Delta$ . By construction, this theory is explicitly equivariant with respect to translations and rotations but also turns out to be explicitly Galilean-invariant, as it should. Not only is the resulting description more accurate and general than state-of-the-art LES models, it is explicit and easily interpretable, which allows one to make specific predictions. For example, at scales  $\Delta$  small compared to the size of large-scale coherent structures, the energy flux is dominated by the contribution from the  $C$  tensor and scales as  $\Delta^4$ , which is not directly implied by the fundamental model (1).

It is worth emphasizing that the data-driven framework described in this letter requires a minimal number of ingredients—the fundamental model (which could also be derived in a data-driven way [26]), some of the fundamental symmetries of the problem, and dimensional analysis—and no specific phenomenological assumptions. Hence, it should readily generalize to other multiscale problems with polynomial nonlinearities.

*Acknowledgments*—This work was supported by the Defense Advanced Research Projects Agency (DARPA).

*Comp. Phys.* **318**, 22 (2016).

- [13] M. Schmelzer, R. Dwight, and P. Cinnella, Data-driven deterministic symbolic regression of nonlinear stress-strain relation for RANS turbulence modelling, in 2018 Fluid Dynamics Conference, p. 2900 (2018).
- [14] K. Jakhar, Y. Guan, R. Mojgani, A. Chattopadhyay, and P. Hassanzadeh, Learning closed-form equations for subgrid-scale closures from high-fidelity data: Promises and challenges, *JAMES* **16**, e2023MS003874 (2024).
- [15] J. Weatheritt and R. D. Sandberg, The development of algebraic stress models using a novel evolutionary algorithm, *Int. J. Heat Fluid Flow* **68**, 298 (2017).
- [16] M. Reissmann, J. Hasslberger, R. D. Sandberg, and M. Klein, Application of gene expression programming to a-posteriori LES modeling of a Taylor-Green vortex, *J. Comp. Phys.* **424**, 109859 (2021).
- [17] A. Ross, Z. Li, P. Perezhigin, C. Fernandez-Granda, and L. Zanna, Benchmarking of machine learning ocean subgrid parameterizations in an idealized model, *JAMES* **15**, e2022MS003258 (2023).
- [18] M. E. Pessah, C.-K. Chan, and D. Psaltis, The signature of the magnetorotational instability in the Reynolds and Maxwell stress tensors in accretion discs, *Mon. Not. R. Astron. Soc.* **372**, 183 (2006).
- [19] S. B. Pope, *Turbulent Flows* (Cambridge University Press, 2000).
- [20] P. Sagaut, *Large Eddy Simulation for Incompressible Flows: An Introduction* (Springer, 2006).
- [21] P. Y. Chou, On velocity correlations and the solutions of the equations of turbulent fluctuation, *Q. Appl. Math.* **3**, 38 (1945).
- [22] R. A. Clark, J. H. Ferziger, and W. C. Reynolds, Evaluation of subgrid-scale models using an accurately simulated turbulent flow, *J. Fluid Mech* **91**, 1 (1979).
- [23] M. Germano, A proposal for a redefinition of the turbulent stresses in the filtered Navier–Stokes equations, *Phys. Fluids A* **29**, 2323 (1986).
- [24] D. Gurevich, Data-driven inference of symmetry-equivariant models of natural phenomena, Ph.D. thesis, Princeton University (2025).
- [25] M. Golden, R. O. Grigoriev, J. Nambisan, and A. Fernandez-Nieves, Physically informed data-driven modeling of active nematics, *Sci. Adv.* **9**, eabq6120 (2023).
- [26] D. R. Gurevich, M. R. Golden, P. A. Reinbold, and R. O. Grigoriev, Learning fluid physics from highly turbulent data using sparse physics-informed discovery of empirical relations (SPIDER), *J. Fluid Mech* **996**, A25 (2024).
- [27] C. J. Wareing, A. T. Roy, M. Golden, R. O. Grigoriev, and S. M. Tobias, Data-driven discovery of the equations of turbulent convection, *GAFD*, **1** (2025).
- [28] G. Boffetta and R. E. Ecke, Two-dimensional turbulence, *Ann. Rev. Fluid Mech.* **44**, 427 (2011).
- [29] C. Meneveau and J. Katz, Scale-invariance and turbulence models for large-eddy simulation, *Ann. Rev. Fluid Mech.* **32**, 1 (2000).
- [30] S. B. Pope, A more general effective-viscosity hypothesis, *J. Fluid Mech* **72**, 331 (1975).
- [31] S. Ghosal, T. S. Lund, and P. Moin, A local dynamic model for large eddy simulation, *Annual Research Briefs*, **1992** (1993).
- [32] A. Leonard and G. Winckelmans, A tensor-diffusivity subgrid model for large eddy simulation, in Proc. Isaac Newton Institute Symposium/ERCOFTAC Workshop, p. 147 (1999).

- [33] C. G. Speziale, S. Sarkar, and T. B. Gatski, Modelling the pressure-strain correlation of turbulence: an invariant dynamical systems approach, *J. Fluid Mech.* **227**, 245 (1991).

*End Matter*—To illustrate how our approach and the effective field theory introduced here fit in the mature field of turbulence modeling, we draw some parallels with phenomenological modeling approaches and models and provide a more comprehensive comparison of our results with those of the leading LES models. Specifically, we use the dynamic Smagorinsky (DS) model and the dynamic mixed (DM) model, neither of which describes subgrid scales explicitly and assumes the SGS to be a function of large (resolved) scales only. The DS model uses the eddy viscosity assumption

$$\tau_{ij} = \nu_e \bar{S}_{ij}, \quad \nu_e = -2 (c_{\text{smg}} \Delta)^2 |\bar{S}| \quad (12)$$

where  $c_{\text{smg}}$  is a nondimensional scalar field determined by a dynamic procedure [6]. The DM model is a hybrid between a similarity model and the DS model:

$$\tau_{ij} = c_{\text{sim}} (\tilde{u}_i \tilde{u}_j - \bar{u}_i \bar{u}_j) - 2 (c_{\text{smg}} \Delta)^2 |\tilde{S}| \tilde{S}_{ij}, \quad (13)$$

where the tilde and overbar describe filtering at cut-off scales  $\Delta$  and  $\gamma\Delta$  respectively. In this paper, the DM model was employed with  $c_{\text{sim}} = \gamma = 1$  [29], in which case the first term on the right-hand-side of equation (13) corresponds to the Leonard stress tensor ( $L$ ) and the second to the DS model. The DS model, as well as its implementation within the DM model, employs local averaging with a Gaussian kernel at the test filter width,  $\gamma\Delta$  [31].

As mentioned previously, the parameterization of the SGS stress tensor inferred from the data has a direct connection to the formal series expansions of the component tensors  $L$  and  $C$  in powers of  $\Delta$ . One finds  $L = O(\Delta^2)$ ,  $C = O(\Delta^4)$  and  $R = O(\Delta^6)$ , so  $L$  provides the dominant contribution to  $\tau$ , with  $C$  and  $R$  serving as progressively smaller corrections. Keeping just the first right-hand-side term in equation (7) yields the nonlinear/gradient model [32] that was recently rediscovered using a data-driven approach [14]. This is the leading-order term in the series expansion of  $L$ ; hence, we will refer to the corresponding parameterization as the L model. Recall that the sum of the first and second terms corresponds to the two leading-order terms in the series expansion of  $L + C$ . Hence, we will refer to this parameterization as the LC model; it has no analogue in the LES/RANS literature.

The governing equation (10) for the Reynolds tensor, which appears in the LCR model, has no direct analogues in LES and RANS literature either. It does, however, contain several terms found in the evolution equations which appear in RANS models, e.g., SSG [33] and its variants, notably the advection term  $\bar{u}_k \nabla_k R_{ij}$  and the production term(s)  $R_{ik} \nabla_k \bar{u}_j + R_{jk} \nabla_k \bar{u}_i$ . In fact, equation (10) can be written in a much simpler form

$$\bar{R}_{ij} = \nu \nabla^2 R_{ij} - \frac{1}{2} |\bar{S}| R_{ij}, \quad (14)$$

where

$$\bar{R}_{ij} = \partial_t R_{ij} + \bar{u}_k \nabla_k R_{ij} - R_{ik} \nabla_k \bar{u}_j - R_{jk} \nabla_k \bar{u}_i \quad (15)$$

is known as the upper-convected or Oldroyd time derivative.

To compare the accuracy of different models in describing the effect of the subgrid scales, it is useful to consider several different metrics. The accuracy with which the SGS stresses themselves are predicted by a particular LES model can be quantified by the correlation  $C_\tau = \mathcal{C}(\tau_{\text{DNS}}, \tau_{\text{LES}})$ . As table I illustrates, the DS model fails to predict  $\tau$  with any meaningful accuracy for any flow considered here. The DM model is quite accurate for the flow F3 which features the largest eddies, but its accuracy quickly deteriorates as the size of the eddies decreases (flow F2 and especially flow F1). The accuracy of the L model exceeds that of the DM model slightly for every flow considered (similar performance is not unexpected since  $\tau \approx L$  for both models), with the LC model bringing further improvement in accuracy. The LCR model is not only the most accurate, but its predictions are essentially perfect for all of the flows and values of  $Re$  considered here, with the correlation exceeding 99% in every case.

We next examine the local energy fluxes, as they are extremely important for a proper description of backscatter. We see that LCR is the only model that consistently captures the spatiotemporal structure of the fluxes, with the correlation  $C_\Pi = \mathcal{C}(\Pi_{\text{DNS}}, \Pi_{\text{LES}})$  exceeding 97% in every case (cf. table I), consistent with the results shown in figure 2. The L model is well-known to yield  $\Pi = 0$ , while the accuracy of the LC model trails the LCR model despite reproducing the SGS stress tensor with high precision. This illustrates that high values of  $C_\tau$  are a necessary but not sufficient condition for the accuracy of a SGS parameterization. Both the DS and the DM model completely fail to reproduce the spatiotemporal structure of the energy flux for any of the flows considered here.

Finally, let us consider the net energy flux  $\ell^2 \langle \Pi \rangle$ . For an accurate model, the ratio  $q_\Pi \equiv \langle \Pi_{\text{LES}} \rangle / \langle \Pi_{\text{DNS}} \rangle$  should be near unity (or 100%). Phenomenological models are commonly designed and tuned to reproduce the net energy dissipation. Hence, it is perhaps not surprising that both the DS and the DM model manage to predict the net energy flux for the freely decaying flow (F2) with reasonable accuracy despite completely failing at describing its spatiotemporal structure. However, both phenomenological models overpredict the net flux for the inverse cascade (F1) and severely underpredict it for the direct cascade (F3), raising the question of whether the good agreement for the flow F2 is purely coincidental. The L model cannot predict the net flux, as expected, while the LC model consistently captures only 50% to 80% of the net flux. Once again, the LCR model is the only one able to consistently predict the net flux, which illustrates the importance of including the contribution from the Reynolds stress tensor ( $R$ ) in the parameterization of the SGS stress tensor.

		Re = $10^4$			Re = $10^5$			Re = $10^6$			
		model	F1	F2	F3	F1	F2	F3	F1	F2	F3
$C_\tau$	DS	0.13%	0.01%	0.01%	0.24%	0.01%	0.01%	0.27%	0.01%	0.01%	
	DM	82.28%	99.71%	99.67%	73.52%	96.25%	99.67%	71.44%	96.17%	99.66%	
	L	92.27%	99.27%	99.94%	89.21%	99.15%	99.93%	88.44%	99.14%	99.934%	
	LC	97.70%	99.93%	99.99%	95.94%	99.89%	99.99%	95.40%	99.89%	99.99%	
	LCR	99.47%	99.98%	99.99%	99.34%	99.97%	99.99%	99.33%	99.97%	99.99%	
$C_\Pi$	DS	26.01%	24.86%	22.77%	26.28%	27.87%	24.05%	22.48%	30.63%	24.06%	
	DM	27.62%	18.00%	15.64%	29.63%	20.20%	13.41%	27.03%	21.08%	13.40%	
	L	0%	0%	0%	0%	0%	0%	0%	0%	0%	
	LC	83.49%	90.57%	99.44%	75.41%	83.81%	94.12%	72.26%	83.07%	93.98%	
	LCR	96.85%	98.02%	99.85%	96.97%	97.52%	98.89%	97.12%	97.40%	98.83%	
$q_\Pi$	DS	131.76%	107.25%	31.53%	129.05%	106.27%	26.87%	128.74%	106.17%	26.86%	
	DM	134.12%	109.92%	35.03%	131.36%	108.93%	30.19%	131.04%	108.83%	30.18%	
	L	0%	0%	0%	0%	0%	0%	0%	0%	0%	
	LC	59.31%	69.83%	82.33%	49.13%	62.29%	58.60%	46.33%	60.78%	56.28%	
	LCR	104.18%	104.63%	103.38%	103.81%	104.08%	104.94%	102.71%	103.93%	104.63%	

TABLE I: The accuracy of the SGS stresses and corresponding energy fluxes for flows F1–F3, with  $R$  computed from DNS. To test the limits of the inferred parameterization, we purposely chose a coarse resolution with a cutoff scale  $\Delta = \ell/64$  that is close to the size of the eddies in the flow F1. Perfect accuracy corresponds to 100%.